IMAGE RECONSTRUCTION IN PET

RECONSTRUCCIÓN DE IMÁGENES EN TEP

Richard Laforest

Washington University School of Medicine, Mallinckrodt Institute of Radiology, St.Louis, USA

(Recibido: Marzo/2015. Aceptado: Julio/2015)

Abstract

In this paper we review the basics of PET and discuss the fundamental principle of the physics of PET, the detection of photons and the creation of sinograms. The principles of PET image formation as described with the presentation of the basic back-projection technique and the now well established statistical iterative image reconstruction technique. We also discuss the implementation of the positron range correction and the inclusion of the time-of-flight information for the purpose of improve image contrast and signal to noise.

Keywords: PET, backprojection, statistical reconstruction, positron range, time of flight

Resumen

En este artículo se revisarán las bases físicas de la técnica PET, la detección de fotones y la creación de sinogramas. Junto a los principios de la formación de imágenes PET, se presentarán las técnicas de retroproyección y la técnica de reconstrucción de imágenes estadística iterativa. Adicionalmente, se discutirá la implementación de la corrección del rango del positrón y la inclusión del tiempo de vuelo de la información, esto con el propósito de mejorar el contraste de imágen y ruido de la señal.

Palabras clave: TEP, retroproyección, reconstrucción estadística, rango de positrones, tiempo de vuelo.

Richard Laforest: laforestr@wustl.edu

Introduction

Proton rich nuclides predominantly decay by β^+ decay and Positron Emission Tomography (PET) operates from the simultaneous detection of the two photons arising from the annihilation of the positron in matter. The principle of PET is that spatial localization of a biological molecule labeled with a positron decaying nuclide can be localized from the spatial position of lines adjoining the detection of these photons. This phenomena was initially proposed in the 50′s as planar projection imaging systems but it is only with the advent of tomographic image reconstruction and the development of modern cylindrical PET scanners in the early 70′s that allowed the three dimensional reconstruction of the activity distribution within the living body. This chapter will discuss the fundamentals of image reconstruction employed with PET starting with the basic of back projection techniques as they form the basis for discussion of any reconstruction algorithm. The paper will then describe modern iterative reconstruction algorithms and discuss their implementation and properties.

Fundamentals of PET

Positron decay results in the emission of a positron and a neutrino whose summed energy equals the mass difference between the mother and daughter nuclides minus twice the rest mass of the electron. This energy is shared between the positron, neutrino and recoiling daughter nucleus. Since the daughter nucleus is typically several thousand times heavier than the positron, the energy is essentially divided between the neutrino and positron. The energy distribution of the positron [ref Krane]. Since the positron will be emitted with kinetic energy of several hundreds of keV, the positron will travel some distance in tissue before coming annihilation with an atomic electron. This positron range is dependent upon the decay energy and thus the positron range will be different for different nuclides. For ^{18}F and ^{64}Cu, this range is of the order of 1 mm but for other nuclides such as ^{82}Rb or ^{15}O, the positron range can be as long as 15-20 mm. Positron annihilation typically occurs when the positron has slowed down enough to form a direct annihilation with an atomic electron or to

form a positronium (e^+-e^-). In most instances (99.75%), positron annihilation will result in the emission of two annihilation photon emitted back-to-back with equal energy of 511 keV.

A PET camera will thus aim at detecting these two annihilation photons and provide information about the spatial location of the point of detection of these photons in the PET detectors. The most widely used configuration of PET scanner is with the cylindrical geometry with, for example in the case of human whole-body scanners, with 80 cm detector radius and 15-25 cm axial field of view (FOV). The cylindrical PET arrangement is typically composed of individual block detectors covering the surface of the cylinder. Each block, themselves being made of an array of scintillation crystals with scintillation read out by an array of photo-multiplier tubes or a single position sensitive photo-multiplier tube. Typically, arrangement of PET detector blocks are essentially optimized to match the imaging application at hand. For human imaging, typically 3-4 rings of 56-60 detector blocks made of 8x8 arrays of 4mm crystal will provide the spatial coverage for a $\sim$20 cm axial field of view.

The PET scanner will essentially collect events for which two photons are detected within a coincidence window and the position of detection of these photon within the PET ring will form a line of response. Since typical PET scanners contains 20-30 thousand crystals, several millions of lines of response are possible. The collection of the number of counts for each line of response is organized as sinogram and will be discussed further below.

Three types of events are typically recorded. True coincidences are formed by the coincident detection of un-scattered annihilation photons arising from a single positron decay. Scatter coincidence arising when one or the two photons undergo Compton scattering within the subject, and finally a Random coincidences can be formed if two positron decay occur sufficiently close in time and where one the two photons from each decay is detected in coincidence. Only the True coincidences are useful for image formation and thus correction for Scatter and Randoms is typically performed, along as correction for attenuation.

A fully 3D scanner will this collect an enormous amount of lines of response and historically older generation of scanner utilize septas (or thin sheet of lead collimator) between each crystal rings. These septas had for function to limit the collection of line of response perpendicular of the field of view and also provided the benefit of reducing the collection of scatter. These septas conferred the appellation of ′2D′ PET scanners despite the fact that both scanners working with or without septas can produce three-dimensional images of the activity distribution. With the advent of faster scanner electronic and faster computers for image reconstruction, septas have been eliminated by most vendors.

Data organization

As described above, a line of response is the formed by the line joining two individual crystals in the PET scanners forming a coincidence event. The number of coincidence within each line of response is a measure of the line integral of the number of annihilation events occurring along each line of response. The most widely employed data model is through the sinogram defined as a three dimensional matrix whose axis represent the projection bin, view angle and axial position. Figure 1 illustrate the concept of this memory organization. Each projection line (dotted line) represents an integration of the activity concentration along particular direction as defined by the scintillation crystals participating in this coincidence event.

Image Reconstruction

PET image reconstruction can be divided in essentially two classes: analytical and iterative. The most employed analytical technique is certainly the back projection algorithm and it is thus a natural place to start the discussion as it form the basis for many other image reconstruction techniques.

Filtered Back Projection. The process of data collection described above can be seen an operation of forward projection (i.e. line integral through image space) along predefined orientation. Mathematically, this operation is referred as the Radon transform.

The back-projection algorithm thus simply back-project in image space the collected coincidence along each line of response. Summing all these inverse Radon transformation, will thus yield to overlapping back-projection and formation of an image of the activity distribution. This simple linear superposition of backprojection will lead to 1/r blurring and this blurring effect is typically prevented by the application of the ramp filter which increases the intensity of the high-frequency component (sharper images). Thus the algorithm of Filtered Back Projection (FBP) will proceed by 1) Taking the Fourier Transform of a given projection, 2) Multiplying by the ramp filter, 3) Taking the inverse Fourier Transform, and 4) Back-projecting through the image volume. The process is then repeated for each slice.

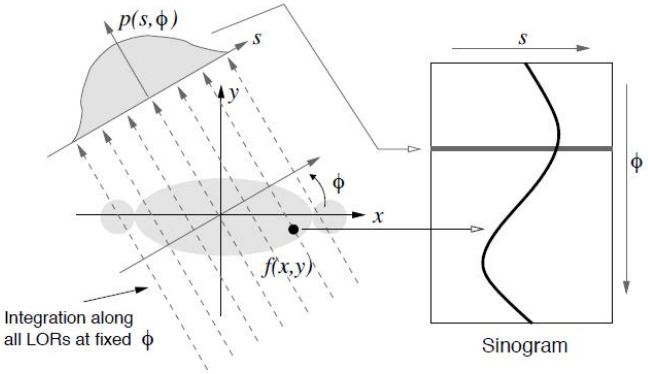

FIGURE 1. *Principle of linear integration along parallel lines of response and data organization in sinograms.*

Although very fast and quantitative, i.e. the intensity in the image is unbiased, FBP images will typically be noisy as noise in the sinograms will propagate directly to the images. Statistical iterative reconstruction technique have now taken the place as they allow to both reduce image noise and improve resolution.

Iterative Reconstruction. The forward projection operator can be defined as a two dimensional matrix whose column element corresponds to each pixel in the image volume, and where each line element represent each line of response. If we represent, the

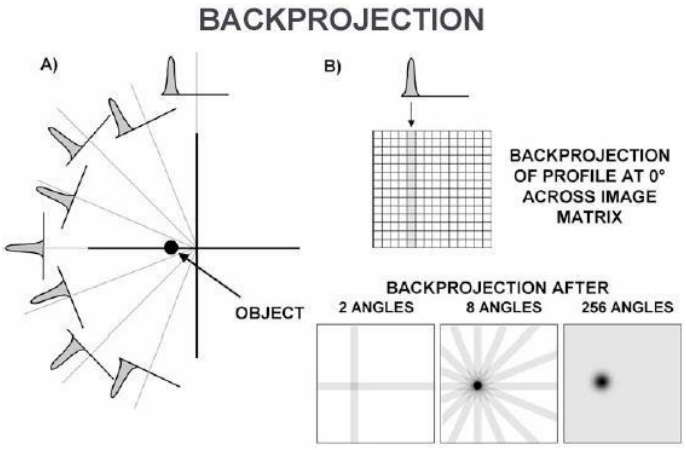

FIGURE 2. *Principle of backprojection algorithm. Taken form Cherry, Sorensen and Phelps, Physics in Nuclear Medicine, 3rd Edition, 2003.*

image space as X_i, where i is the index of each image pixel, and Yj the sinogram element j, then we can define the forward projection operation as

$$Y_j = \sum_{i,j} H_{ij} X_i \tag{1}$$

In the absence of randoms, scatter and noise X_i can be deterministically calculated by the inversion of the matrix operation. For a noiseless image, this equation can be inverted to yield

$$X = \left(\mathbf{H}^T \mathbf{H}\right)^{-1} \mathbf{H}^T \mathbf{Y} \, (2) \tag{2}$$

where we have employed the matrix notation.

However, in this algebraic technique, the noise is stochastic and error in the Randoms and Scatter evaluation will lead to an ill-posed problem, i.e. small perturbation due to noise will leads to large fluctuation in the image estimated.

Typically, the solution X_i is determined by using iterative techniques. The idea of iterative statistical image reconstruction is to find the best representation of the activity distribution than can match the measured projection data based on the knowledge of the system model (scanner response), physics of positron decay,

statistical model (Poisson decay), and while accounting for Scatter, attenuation and Randoms. Typically, such algorithm will be characterized by five elements: 1. Data model, 2. System model, 3. Measurement statistical model, 4. Cost function and 5. The algorithm to reach the solution. We will discuss these in turns. *Data model.* For most algorithm, the continuous image space is sampled on discrete abutting voxels centered on equally spaced gridding points. Other data model found will be with spherically overlapping blobs (RAMLA).

System Model. The system model is the operator defined in equation 1. For a typical scanner, the number of image voxels is of the order of several millions and several hundred million lines of response. Each element of this matrix represents the probability of detection of in pixel X_i in the line of response Y_j. This matrix is usually very sparse and can be reduced in size by using the symmetries in the scanner design. This matrix can be calculated on the fly with simple approximations or pre-calculated and stored as a system matrix. In this case, typically the scanner geometry and its resolution effect as well as the fundamental physics of positron decay can be included in the system model. These approaches can therefore lead to resolution recovery where the loss of resolution due to crystal size, crystal penetration (parallax), photon non-acolinearity and positron range can be (at least partially) recovered. Q$_i$ and Leahy developed a factored approach for the calculation of the system matrix and using the Maximum a posteriori approach.

Statistical Model. Radioactive decay obeys Poison distribution defined by

$$P\left(Y\right) = \frac{\lambda_i^{y_i} e^{-\lambda_i}}{y_i!} \tag{3}$$

where, $\lambda_i = \sum_j H_{ij} X_j + \text{Random}_i + \text{Scatter}_i$ the estimated number of counts in sinogram element i from the activity in voxel j, and y_i is the measured counts in the sinogram element i. From this we can derive the likelihood function, where the statistically most probable solution is the one for which the likelihood is maximal. More conveniently, the log of the likelihood function is estimated.

$$L\left(P\left(Y\right)\right) = \prod_{i=1}^{M} \frac{\lambda_i^{y_i} e^{-\lambda_i}}{y_i!} \tag{4}$$

More conveniently, the log of the likelihood function is estimated:

$$L\left(X|Y\right) = \sum_j log\left(\sum a_{ij} X_i + r_j + s_j\right) - \left(\sum_i a_{ij} X_i + r_j + s_j\right) - log\left(y_j!\right) \tag{5}$$

Cost Function. The Maximum Likelihood solution for the equation above will be determined iteratively by the algorithm below but mathematical convergence will take thousands of iterations and may eventually lead to noisy images. In practice, some form of regularization is employed. This can take the form of early termination, application of global smoothing on the resulting images, application of a penalty term that limits to image solutions that are smoother.

Algorithm. To maximization of the log-likelihood function is achieved by the Expectation-Maximization Algorithm defined as:

$$x_j^{n+1} = \frac{x_j^n}{\sum_i P_{ij}} \sum_i \frac{P_{ij} y_i}{\sum_k P_{ik} x_j^n + s_j + r_j} \tag{6}$$

This algorithm essentially forward project an estimate of the activity distribution, add the measured or pre-calculated Scatter and Random, divide from the measured data y_i and then back-project the ratio to image space to finally update the image estimate by multiplication. Starting from a uniform image of 1 throughout time imaging volume, the final image can be obtained in a few successive multiplicative iterations.

The bottleneck for reconstruction speed is the size of the system matrix and event through the use of symmetries, reconstruction time are still fairly long. Fourier rebining technique (FORE) and Ordered subsets are techniques that are commonly employed to reduce reconstruction time. In Fourier rebining, (FORE), fully 3D sinograms are converted to transverse only sinograms. This steps is relatively fast and allow to perform iterative reconstruction on transverse planes only which allow for very fast reconstruction. However, these techniques can lead to loss of resolution and image bias. More commonly, order subsets will be used and

allows to reach a satisfactory images in a few iteration only. Development of faster CPU and affordable computer with more memory, and the availability of GPU (Graphical Processing Unit) have led to fast implementation of 3D iterative algorithms that allows for image reconstruction in a practical time of a few minutes.

Positron Range Correction Such iterative algorithm allows a natural framework to include correction for the loss of resolution due to the positron range by including a component of the system model that correspond the blurring due to the positron travel prior to annihilation. These kernels can be calculated by electron transport simulation with codes such as EGSNRC, GEANT, Penelope and others for different media and different nuclides. Such distance are plotted for a few copper isotopes in the Figure 3 below. Using such kernel, we had implemented correction

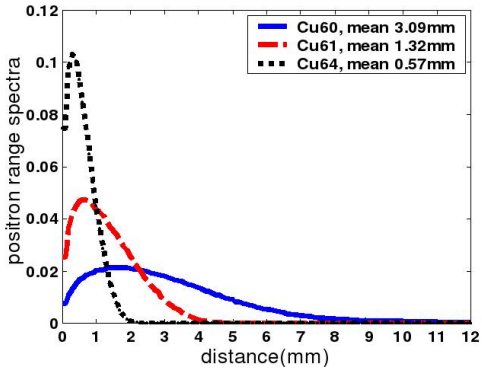

FIGURE 3. ^{60}Cu, ^{61}Cu *and* ^{64}Cu *positron range distribution as calculated with EGSnrc*

for the positron range in MAP algorithm and demonstrated its effectiveness in a series of animal studies. The Figure 4 illustrate the performance of this technique in animal imaging performed with Cu-60, 61 and 64 labeled PTSM which is a blood perfusion agent, i.e. signal intensity in an organ is proportional to its blood supply. Images below are presented for MAP reconstruction (3D iterative reconstruction) with and without range correction. The right side of the figure presents line profiles traced through the kidney to show the increase in resolution where it is observed that less spill-over of

activity is present in the center of the organ as a consequence of the improved resolution.

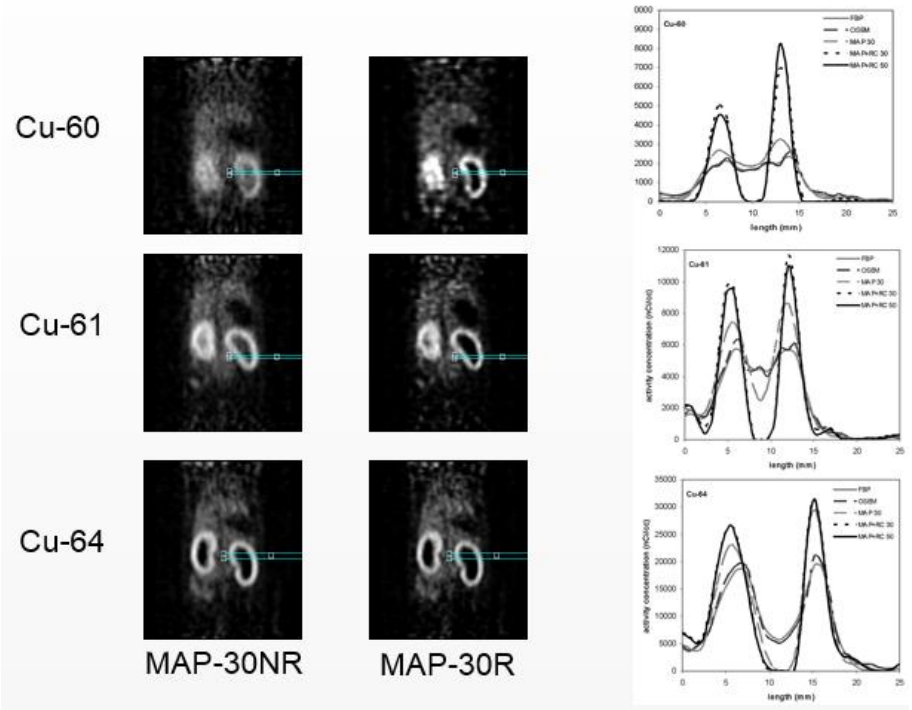

FIGURE 4. *Example of positron range corrected images obtained with* ^{60}Cu*,* ^{61}Cu *and* ^{64}Cu *labeled PTSM. PTSM [1] is a flow agent that will accumulate in region of higher blood flow. Here the animal kidney cortex is seen with the highest activity and the positron range correction illustrated similar qualitative and quantitative activity bio-distribution [2].*

Time of Flight. Time of flight PET proposes to exploit the measured time difference of arrival of the two annihilation photons. For a source located at a distance Δx from the center of the tomograph, a time differential Δt will be observed assuming a perfect temporal resolution from the tomograph. In principle, thus the spatial position of the annihilation point can be entirely determined without the need for the tomographic reconstruction technique described above. In reality, the timing resolution of most PET scanner is of the order of 500ps which leads to a spatial resolution of 7-8 cm. This value is not sufficient to allow for spatial

localization of the activity but can be exploited in the tomography reconstruction algorithm to backproject the activity only in the imaging space defined by the time difference between the arrivals of the two photons as illustrated in Figure 3.

$$\Delta t = \frac{(x + \Delta x)}{c} - \frac{(x - \Delta x)}{c} = \frac{2\Delta x}{c}$$

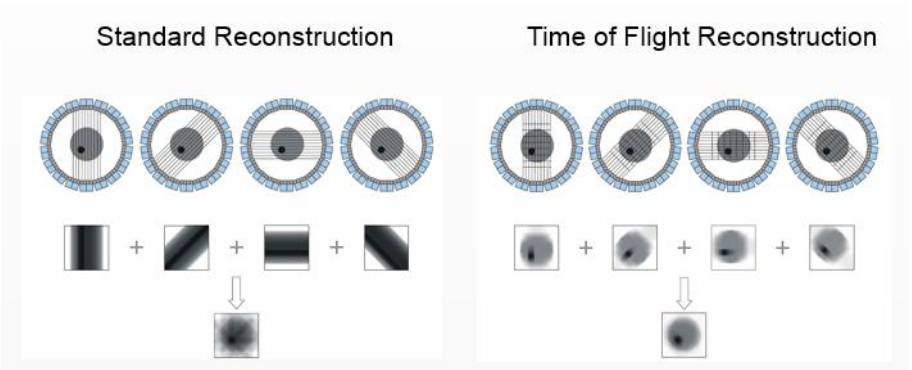

FIGURE 5. *Illustration of the time of flight image reconstruction principle. Taken from Improving PET with HD.PET + Time of Flight (M.Casey, Siemens, available online)*

Conclusions

The advantage of the TOF is thus not in improvement in spatial resolution but in improvement in contrast and signal to noise where larger benefits have been observed for larger patients. This is of significance since larger patients datasets suffer from increased scatter and attenuation and therefore image quality improvement is much needed in those cases.

Acknowledgments

I wish to thank all from whom I borrowed material and whom have contributed material on the web.

References

[1] H. Shelton, J Nucl Med **20**, 1843 (1989).
[2] A. Ruangma, Nucl. Med. Biol. **33**, 217 (2006).